Available online at www.sciencedirect.com
SCIENCE DIRECT®
Journal of Solid State Chemistry 177 (2004) 2058–2067
JOURNAL OF SOLID STATE CHEMISTRY
http://elsevier.com/locate/jssc

A novel open-framework with non-crossing channels in the uranyl vanadates $A(UO_2)_4(VO_4)_3$ (A = Li, Na)

S. Obbade,* C. Dion, M. Rivenet, M. Saadi, and F. Abraham

Laboratoire de Cristallochimie et Physicochimie du Solide, UPRES A 8012, ENSCL et USTL, B.P. 108, F-59652 Villeneuve d'Ascq Cedex, France

Received 26 November 2003; received in revised form 23 January 2004; accepted 1 February 2004

Abstract

A new sodium uranyl vanadate $Na(UO_2)_4(VO_4)_3$ has been synthesized by solid-state reaction and its structure determined from single-crystal X-ray diffraction data. It crystallizes in the tetragonal symmetry with space group $I4_1/amd$ and following cell parameters: $a = 7.2267(4)$ Å and $c = 34.079(4)$ Å, $V = 1779.8(2)$ Å^3, $Z = 4$ with $\rho_{mes} = 5.36(3)$ g/cm^3 and $\rho_{cal} = 5.40(2)$ g/cm^3. A full-matrix least-squares refinement on the basis of F^2 yielded $R_1 = 0.028$ and w$R_2 = 0.056$ for 52 parameters with 474 independent reflections with $I \geqslant 2\sigma(I)$ collected on a BRUKER AXS diffractometer with Mo$K\alpha$ radiation and a CCD detector. The crystal structure is characterized by $^2_\infty[(UO_2)_2(VO_4)]$ sheets parallel to (001) formed by corner-shared UO_6 distorted octahedra and V(2)O_4 tetrahedra, connected by V(1)O_4 tetrahedra to $^1_\infty[UO_5]^{4-}$ chains of edge-shared UO_7 pentagonal bipyramids alternately parallel to the a- and b-axis. The resulting three-dimensional framework creates mono-dimensional channels running down the a- and b-axis formed by face-shared oxygen octahedra half occupied by Na. The powder of Li analog compound $Li(UO_2)_4(VO_4)_3$ has been synthesized by solid-state reaction. The two compounds exhibit high mobility of the alkaline ions within the two-dimensional network of non-intersecting channels.

Keywords: Uranyl vanadate; Solid-state synthesis; Crystal structure refinement; Non-crossing mono-dimensional channels; Cationic conductivity

1. Introduction

Uranyl-containing oxides have been the focus of considerable interest in recent years due to their important environmental aspect and the possibility of their applications in the nuclear industry. Moreover, their structural chemistry is very exciting, in particular the association of uranyl ions with oxoanions-containing transition metals in their highest possible oxidation states (V, Nb, Mo, W, etc.) allowed the synthesis of many compounds with complex and varied crystal structures. The structural diversity of the obtained compounds is related to the variety of different coordination polyhedra about U(VI) (hexagonal bipyramid, pentagonal bipyramid, distorted octahedron) and about the transition metal ion (tetrahedron, square pyramid, octahedron) and to the huge possibilities of linkages between these polyhedra. Most of these linkages lead to the building of layers as evidenced in a comparison and a hierarchy of crystal structure of U(VI) minerals and inorganic compounds reported by Burns et al. [1]. In alkaline-containing layered compounds the alkaline ions occupy the interlayer space displaying high mobility and leading to good electrical conductivity [2,3]. All the alkaline uranyl vanadates known today are layered compounds and this family magnificently illustrates the variety of coordination geometries and the flexibility of the linkage between polyhedra. Many belong to the large class of compounds with general formula $M^{n+}_{2/n}(UO_2)_2V_2O_8{\cdot}xH_2O$, where M can be most mono, di, or trivalent cations [2–11], and adopt the structure of the carnotite mineral $K_2(UO_2)_2V_2O_8{\cdot}xH_2O$, an uranyl ore. These materials are characterized by $^2_\infty[(UO_2)_2V_2O_8]^{2-}$ sheets built edge and corner-shared UO_7 pentagonal bipyramids linked by $V_2O_8^{6-}$ units. While the $V_2O_8^{6-}$ groups are formed by two inverse VO_5 square pyramids sharing an edge. The $^2_\infty[(UO_2)_2V_2O_8]^{2-}$ sheets are held together by interlayer cations alone or surrounded by water molecules. In $CsUV_3O_{11}$ [12], the $^2_\infty[(UO_2)(VO_3)_3]^-$ layers result from the linkage of UO_8 hexagonal bipyramids and VO_5 square pyramids sharing edges and corners and are similar to the layers found in UV_3O_{10} [13]; in fact the

*Corresponding author. Fax: +33-320436814.
E-mail address: obbade@ensc-lille.fr (S. Obbade).

0022-4596/$ - see front matter © 2004 Elsevier Inc. All rights reserved.
doi:10.1016/j.jssc.2004.02.011

Table 1
Observed and calculated X-ray powder diffraction pattern for $NaU_5V_3O_{20}$

$h\,k\,l$	$2\theta_{obs}$	$2\theta_{calc}$	I_{obs}/I_o	$h\,k\,l$	$2\theta_{obs}$	$2\theta_{calc}$	I_{obs}/I_o
0 0 4	10.376	10.365	1	0 3 9	44.550	44.558	12
0 1 1	12.512	12.507	15	2 3 1	45.309	45.306	<1
0 1 3	14.523	14.511	9	3 2 3	45.965	45.961	<1
0 1 5	17.882	17.871	23	0 1 17	47.005	47.007	4
1 1 2	18.112	18.109	33	2 3 5	47.255	47.251	2
1 1 4	20.256	20.247	1	0 3 11	47.809	47.805	1
0 0 8	20.816	20.830	4	2 2 12	47.868	47.864	1
0 1 7	21.980	21.993	43	1 3 10	47.904	47.904	5
1 1 6	23.382	23.398	3	1 2 15	48.983	48.979	1
0 2 0	24.625	24.622	100	2 3 7	49.147	49.137	5
0 1 9	26.540	26.553	53	0 2 16	49.648	49.654	7
0 2 4	26.790	26.783	<1	0 4 0	50.493	50.499	13
1 2 1	27.709	27.711	5	1 1 18	51.443	51.437	7
1 2 3	28.683	28.702	3	0 3 13	51.498	51.495	2
1 2 5	30.587	30.596	9	2 3 9	51.574	51.571	4
0 1 11	31.397	31.390	<1	0 4 4	51.705	51.703	1
1 1 10	31.526	31.531	11	1 4 1	52.245	52.242	<1
0 2 8	32.459	32.471	2	0 1 19	52.526	52.533	1
1 2 7	33.243	33.254	13	1 2 17	53.789	53.778	3
2 2 0	35.111	35.106	12	3 3 0	53.803	53.801	1
0 1 13	36.437	36.430	2	1 4 5	54.002	54.000	1
1 2 9	36.523	36.531	14	3 3 2	54.092	54.091	4
2 2 4	36.710	36.704	2	3 3 4	54.955	54.954	1
0 3 1	37.414	37.409	1	1 3 14	55.083	55.094	9
0 3 3	38.179	38.174	1	0 4 8	55.205	55.203	1
0 3 5	39.670	39.665	11	1 4 7	55.710	55.719	4
1 3 2	39.776	39.780	17	2 2 16	56.194	56.193	3
1 1 14	41.048	41.042	13	3 3 6	56.374	56.373	<1
2 2 8	41.183	41.178	1	1 1 20	56.931	56.929	3
0 1 15	41.645	41.640	2	2 4 0	56.970	56.969	8
0 3 7	41.816	41.819	7	1 4 9	57.942	57.954	5
0 0 16	42.406	42.405	11	0 1 21	58.231	58.229	2
1 3 6	42.630	42.626	1	1 2 19	58.850	58.849	1

Note: $\lambda = 1.54056$ Å, refined zero-point correction $-0.006(2)$ for θ; $a = 7.2215(5)$ Å, $c = 34.067(2)$ Å; $F_{20} = 135$ (0.0059; 25).

Table 2
Observed and calculated X-ray powder diffraction pattern for $LiU_5V_3O_{20}$

$h\,k\,l$	$2\theta_{obs}$	$2\theta_{calc}$	I_{obs}/I_o	$h\,k\,l$	$2\theta_{obs}$	$2\theta_{calc}$	I_{obs}/I_o
0 0 4	10.500	10.492	3	2 3 1	45.210	45.206	1
0 1 1	12.477	12.492	14	2 3 3	45.882	45.878	1
0 1 3	14.536	14.543	7	2 3 5	47.203	47.199	3
0 1 5	17.974	17.969	8	0 1 17	47.541	47.543	3
1 1 2	18.100	18.095	38	0 3 11	47.965	47.963	2
0 0 8	21.066	21.081	2	3 1 10	48.018	48.015	5
0 1 7	22.160	22.162	46	2 2 12	48.070	48.072	2
1 1 6	23.503	23.498	12	2 3 7	49.134	49.130	7
0 2 0	24.581	24.572	100	1 2 15	49.354	49.353	1
0 1 9	26.804	26.792	47	0 2 16	50.091	50.087	11
1 1 8	27.420	27.404	2	0 4 0	50.381	50.383	13
1 2 1	27.645	27.657	5	0 4 2	50.697	50.693	1
1 2 3	28.666	28.672	2	0 4 4	51.618	51.617	8
1 2 5	30.607	30.612	11	2 3 9	51.618	51.621	8
0 1 11	31.704	31.701	9	0 3 13	51.730	51.728	2
1 1 10	31.764	31.775	9	1 1 18	51.994	51.992	4
0 2 8	32.600	32.596	1	1 4 1	52.124	52.127	1
1 2 7	33.328	33.329	16	1 4 3	52.713	52.729	2
2 2 0	35.019	35.030	16	0 1 19	53.160	53.151	2
2 2 9	36.682	36.668	20	3 3 0	53.679	53.676	2
1 2 9	36.682	36.673		4 1 5	53.927	53.925	2
0 1 13	36.816	36.814	2	3 3 2	53.976	53.973	4
0 3 1	37.334	37.330	2	1 2 17	54.234	54.236	3
0 3 3	38.128	38.114	2	0 2 18	55.217	55.217	2
0 3 5	39.646	39.642	3	1 3 14	55.351	55.355	12
3 1 2	39.688	39.703	22	4 1 7	55.688	55.685	5
2 2 8	41.249	41.245	2	3 3 6	56.313	56.311	1
1 1 14	41.432	41.437	14	2 2 16	56.558	56.563	4
0 3 7	41.845	41.846	8	2 4 0	56.825	56.835	10
0 1 15	42.099	42.098	1	2 4 2	57.124	57.121	2
1 3 6	42.630	42.618	2	2 4 4	57.970	57.974	6
0 0 16	42.926	42.928	8	1 4 9	57.970	57.977	
0 3 9	44.645	44.646	12	3 3 8	58.307	58.305	1
1 2 13	44.768	44.766	2	0 1 21	58.929	58.935	2

Note: $\lambda = 1.54056$ Å, refined zero-point correction $-0.003(1)$ for θ; $a = 7.2379(5)$ Å, $c = 33.677(2)$ Å; $F_{20} = 130$ (0.0053; 29).

layers can be described by VO_5 pyramids sharing corners, the obtained $^2_\infty[VO_3]^-$ layers create equilateral triangles and hexagons, the hexagon centers are occupied by linear uranyl ions perpendicular to this plane. In $M_6(UO_2)_5(VO_4)_2O_5$ with M = Na, K, Rb [14,15] the layers are built up from VO_4 tetrahedra, UO_7 pentagonal bipyramids and UO_6 distorted octahedra. The UO_7 pentagonal bipyramids share two edges of equatorial pentagons creating zig-zag infinite chains $^1_\infty[UO_5]^{4-}$ connected together by the remaining oxygen atoms of the equatorial pentagons to form $^1_\infty[U_5O_{21}]^{12-}$ ribbons, three uranium polyhedra in width. The ribbons are linked by VO_4 tetrahedra. Depending the orientation of successive VO_4 tetrahedra the formed $^2_\infty[(UO_2)_5(VO_4)_2O_5]^{6-}$ layers are flat or corrugated. Similar $^1_\infty[UO_5]^{4-}$ chains are found in different uranyl vanadates UVO_5 [7], $U_2V_2O_{11}$ [16,17] and $(UO_2)_3(VO_4)_2{\cdot}5H_2O$ [18] where they are linked by VO_5 square pyramids, V_2O_7 divanadate units and VO_4 tetrahedra, respectively.

Finally, in $Cs_4[(UO_2)_2(V_2O_7)O_2]$ layers are built from chains of corner-shared UO_6 distorted octahedra connected by divanadate V_2O_7 units [19].

In this paper we report the synthesis and structure of a sodium uranyl vanadate characterized by a novel framework with a two-dimensional system of non-crossing channels. The synthesis of the Li-analog is also reported and the conductivity properties of these two compounds are compared with other fast lithium or sodium ion conductors.

2. Experimental

2.1. Synthesis

Single crystals of $Na(UO_2)_4(VO_4)_3$ were obtained during the study of the ternary diagram V_2O_5–UO_3–Na_2O by a solid-state reaction between V_2O_5 (Aldrich),

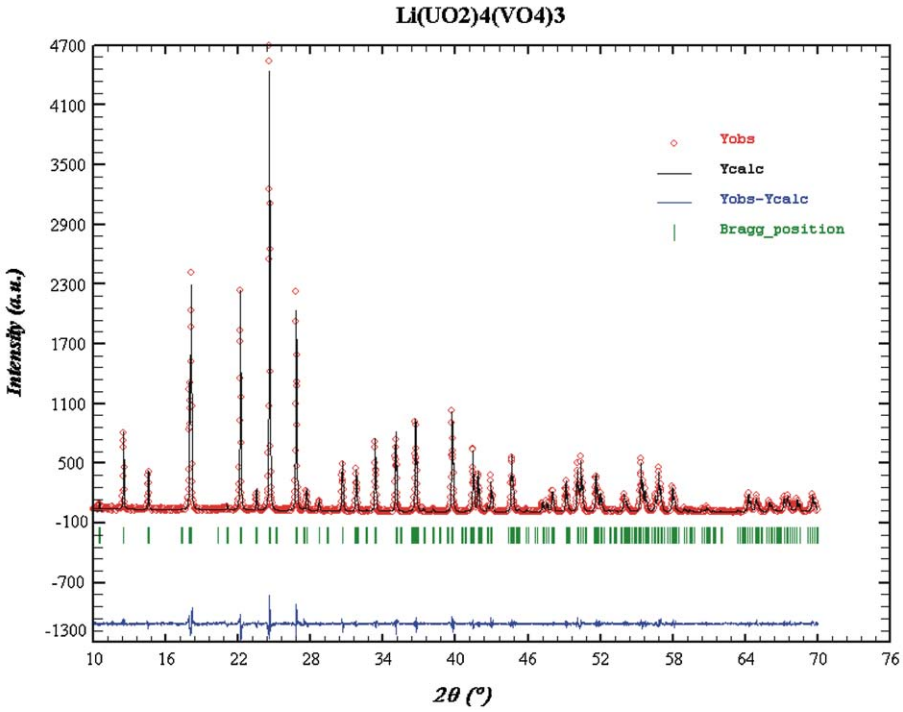

Fig. 1. Observed (Y_{obs}), calculated (Y_{cal}) and difference profiles (($Y_{obs}-Y_{cal}$) from Rietveld refinement of X-ray powder diffraction data of $Li(UO_2)_4(VO_4)_3$ compound. Allowed reflections are indicated by vertical lines.

U_3O_8 (Prolabo) and Na_2CO_3 (Aldrich) mixed in the molar ratio 4:11/3:1, to synthesize single crystals of the suppose phase $Na_2(UO_2)_{11}(VO_4)_8$. The mixture was heated in air at 650°C for 2 days in a platinum crucible with an intermediate grinding. The as-prepared powder was melted at 920°C and cooled at the rate of 3°C/h–500°C and finally at 10°C/h to room temperature. Washing of the obtained yellowish shiny crystalline product with ethanol allowed the separation of yellow single crystals of $Na(UO_2)_4(VO_4)_3$. Attempts to grow single crystals of $Li(UO_2)_4(VO_4)_3$ suitable for single-crystal X-ray diffraction failed.

Pure polycrystalline samples of $M(UO_2)_4(VO_4)_3$ (M= Li, Na) were also prepared by conventional solid-state reactions, using pure initial materials M_2CO_3 (Adrich), U_3O_8 (Prolabo) and V_2O_5 (Aldrich) according to the following reaction:

$$M_2CO_3+8/3U_3O_8+3V_2O_5+4/3O_2 \xrightarrow[\text{one week}]{670^\circ C} 2M(UO_2)_4(VO_4)_3+CO_2,$$

M= Li, Na.

The homogeneous mixture was slowly heated up to 670°C in a platinum crucible and maintained at this temperature during 1 week with intermediate grindings and finally slowly cooled to room temperature. The X-ray powder diffraction pattern of the Na-containing compound is identical to that of crushed single crystals and to that of the calculated pattern from the crystal structure results. The unit cell parameters for both compounds were refined by a least-squares procedure from the indexed powder diffraction patterns recorded, at room temperature, with a Siemens D5000 diffractometer equipped with a secondary monochromator and corrected for $K\alpha_2$ contribution in Bragg–Brentano geometry, using Cu$K\alpha$ radiation in steps of 0.02° and a counting time of 40 s per step, within an angular range of 5–110° in 2θ. The refined unit cell parameters and the indexed powder patterns, with their merit factors F_{20} defined by Smith and Snyder [20] are given in Tables 1 and 2 for $Na(UO_2)_4(VO_4)_3$ and $Li(UO_2)_4(VO_4)_3$, respectively. For $Li(UO_2)_4(VO4)_3$ compound, Fig. 1 shows the good agreement between observed and calculated powder X-ray diffraction diagrams.

The density measured with an automated Micromeritics Accupy 1330 helium pycnometer using a 1-cm^3 cell, indicates a good agreement between the calculated and measured densities, with four formulas per unit cell ($\rho_{mes} = 5.36(3)$ g/cm^3, $\rho_{cal} = 5.40(2)$ g/cm^3 and $\rho_{mes} = 5.31(3)$ g/cm^3, $\rho_{cal} = 5.34(2)$ g/cm^3 for $Na(UO_2)_4(VO_4)_3$ and $Li(UO_2)_4(VO_4)_3$, respectively).

2.2. Single-crystal X-ray diffraction and structure determination

For the sodium compound a well-shaped yellow crystal (0.064, 0.154, 0.034 mm) was selected for X-ray

Table 3
Crystal data, intensity collection and, structure refinement parameters for $Na(UO_2)_4(VO_4)_3$

Crystal data				
Crystal symmetry	Tetragonal			
Space group	$I4_1/amd$			
Unit cell	$a = 7.2267(4)$ Å			
	$b = 7.2267(4)$ Å			
	$c = 34.079(4)$ Å			
	$V = 1779.8(2)$ Å^3			
Z	4			
Chemical formula weight	1447.93 g/mol			
Calculated density	$\rho_{cal} = 5.40(2)$ g/cm^3			
Measured density	$\rho_{mes} = 5.36(3)$ g/cm^3			
Data collection				
Temperature (K)	293(2)			
Equipment	Bruker SMART CCD			
Radiation Mo$K\alpha$	0.71073 Å			
μ (cm^{-1})	378.85			
Crystal imiting faces and distances (mm)	1 0 0	0.032	−1 0 0	0.032
	0 1 0	0.057	0 −1 0	0.057
	0 0 1	0.017	0 0 −1	0.017
Scan mode	ω			
Recording angular range (deg)	2.34–29.28			
Recording reciprocal space	$-9 \leqslant h \leqslant 9$			
	$-9 \leqslant k \leqslant 9$			
	$-45 \leqslant 1 \leqslant 46$			
No. of measured reflections	4683			
R merging factor	0.051			
No. of independent reflections	474			
Refinement				
Refined parameters/restraints	52/0			
Goodness of fit on F^2	1.197			
$R_1[I > 2\sigma(I)]$	0.028			
w$R_2[I > 2\sigma(I)]$	0.056			
R_1 for all data	0.029			
wR_2 for all data	0.057			
Largest diff. Peak/hole(e/Å^3)	2.60/−1.82			

$R_1 = \sum(|F_o| - |F_c|)/\sum|F_o|$.
$wR_2 = [\sum w(F_o^2 - F_c^2)^2/\sum w(F_o^2)^2]^{1/2}$
$w = 1/[\sigma^2(F_o^2) + (aP)^2 + bP]$, where a and b are refinable parameters and $P = (F_o^2 + 2F_c^2)/3$.

Table 4
Atomic positions, equivalent isotropic thermal factors U_{eq} (Å^2) of $Na(UO_2)_4(VO_4)_3$

Atom	Site	Occ.	x	y	z	U_{eq}
U(1)	8*e*	1	1/2	3/4	0.09833(2)	0.0117(2)
U(2)	8*e*	1	0	3/4	0.97375(2)	0.0157(2)
V(1)	8*e*	1	0	3/4	0.06874(8)	0.0113(5)
V(2)	4*b*	1	1/2	1/4	1/8	0.0138(7)
O(1)	8*e*	1	1/2	3/4	0.1534(3)	0.019(3)
O(2)	16*h*	1	0.1916(13)	3/4	0.0959(3)	0.033(3)
O(3)	8*e*	1	1/2	3/4	0.0458(4)	0.028(3)
O(4)	16*h*	1	1/2	0.4462(14)	0.0964(4)	0.036(3)
O(5	16*h*	1	0	0.5720(13)	0.0353(3)	0.033(3)
O(6)	16*h*	1	0.2415(12)	3/4	0.9740(3)	0.039(5)
Na	8*d*	0.5	1/2	1/2	0	0.065(9)

Note: The U_{eq} values are defined by $U_{eq} = 1/3(\sum_i \sum_j U_{ij} a_i^* a_j^* a_i a_j)$.

diffraction investigations. The measurement of X-ray intensities was performed at room temperature using a BRUKER AXS diffractometer equipped with a 1K SMART CCD detector and monochromated Mo$K\alpha$ radiation. Details of the data collection are given in Table 3. Before the crystal structure determination, the

Table 5
Thermal anisotropic displacements for $Na(UO_2)_4(VO_4)_3$ ($Å^2$)

Atom	U_{11}	U_{22}	U_{33}	U_{12}	U_{13}	U_{23}
U(1)	0.0106(5)	0.0138(5)	0.0106(3)	0	0	0
U(2)	0.0277(4)	0.0093(3)	0.0100(3)	0	0	0
V(1)	0.0141(14)	0.0105(13)	0.0103(13)	0	0	0
V(2)	0.0065(10)	0.0065(10)	0.029(2)	0	0	0
O(1)	0.022(10)	0.034(12)	0.000(5)	0	0	0
O(2)	0.014(5)	0.078(8)	0.017(5)	0	−0.001(4)	0
O(3)	0.020(8)	0.027(8)	0.033(9)	0	0	0
O(4)	0.041(6)	0.015(5)	0.056(7)	0	0	0.005(5)
O(5)	0.071(7)	0.009(4)	0.019(5)	0	0	0.001(4)
O(6)	0.028(7)	0.093(11)	0.021(6)	0	0.001(5)	0
Na	0.034(10)	0.063(13)	0.12(2)	0	0	−0.077(14)

Note: The anisotropic displacement factor exponent takes the form $-2\pi^2[h^2a^{*2}U_{11} + k^2b^{*2}U_{22} + l^2c^{*2}U_{33} + \cdots + r + 2hka^*b^*U_{12}]$.

Table 6
Bond distances (Å), angles (deg) and bond valences s_{ij} of $Na(UO_2)_4(VO_4)_3$

U environment

	d_{U-O}	s_{ij}		d_{U-O}	s_{ij}
U(1)–O(3)	1.790(14)	1.653	U(2)–O(6)	1.745(9)	1.803
U(1)–O(1)	1.877(10)	1.404	U(2)–O(6)^{ii}	1.745(9)	1.803
U(1)–O(4)	2.196(10)	0.756	U(2)–O(5)^{iii}	2.347(9)	0.565
U(1)–O(4)^{i}	2.196(10)	0.756	U(2)–O(5)^{iv}	2.347(9)	0.565
U(1)–O(2)	2.230(9)	0.708	U(2)–O(1)^{v}	2.397(10)	0.511
U(1)–O(2)^{i}	2.230(9)	0.708	U(2)–O(5)^{vi}	2.461(10)	0.456
			U(2)–O(5)^{vii}	2.461(10)	0.456
	$\sum s_{ij}$	5.985		$\sum s_{ij}$	6.159

Uranyl ion angles (deg)

O(3)–U(1)–O(1)	180.0(3)
O(6)–U(2)–O(6)^{ii}	179.4(4)

V environment

	d_{V-O}	s_{ij}		d_{V-O}	s_{ij}
V(1)–O(2)	1.666(10)	1.448	V(2)–O(4)^{viii}	1.721(11)	1.251
V(1)–O(2)^{ii}	1.666(10)	1.448	V(2)–O(4)^{ix}	1.721(11)	1.251
V(1)–O(5)^{ii}	1.719(10)	1.255	V(2)–O(4)^{x}	1.721(11)	1.251
V(1)–O(5)	1.719(10)	1.255	V(2)–O(4)^{xi}	1.721(11)	1.210
	$\sum s_{ij}$	5.406		$\sum s_{ij}$	5.004

Na environment

	d_{Na-O}	s_{ij}
Na–O(3)	2.388(9)	0.206
Na–O(3)^{xii}	2.388(9)	0.206
Na–O(6)^{xiii}	2.746(7)	0.078
Na–O(6)^{xiv}	2.746(7)	0.078
Na–O(6)^{xv}	2.746(7)	0.078
Na–O(6)^{xvi}	2.746(7)	0.078
	$\sum s_{ij}$	0.720

Symmetry codes: (i) $1-x, 1.5-y, z$; (ii) $-x, 1, 5-y, z$; (iii) $x, 0.5+y, 1-z$; (iv) $-x, 1-y, 1-z$; (v) $0.75-y, 1.25+x, 0.75+z$; (vi) $-x, 1.5-y, 1+z$; (vii) $x, y, 1+z$; (viii) $0.25+y, 0.75-x, 0.25-z$; (ix) $1-x, 0.5-y, z$; (x) $0.75-y, -0.25+x, 1.25-z$; (xi) $0.25+y, -0.25+x, 0.25-z$; (xii) $1-x, 1-y, -z$; (xiii) $1-x, 1.5-y, -1+z$; (xiv) $x, y, -1+z$; (xv) $x, -0.5+y, 1-z$; (xvi) $1-x, 1-y, 1-z$.

intensity data were corrected for Lorentz, polarization and background effects using the Bruker program SAINT [21]. Then the absorption corrections were computed by the Gaussian face-indexed method with the shape of the crystal using the program XPREP of the SHELXTL package [22], followed by a semi-empirical correction based on redundancy using the SADABS program [23]. The crystal structure was solved in the centrosymmetric $I4_1/amd$ space group, by means of direct methods strategy using SHELXS program [24]

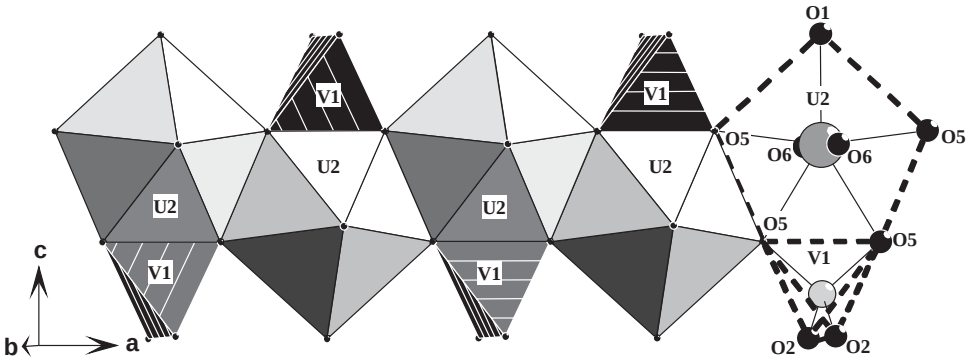

Fig. 2. $U(2)O_7$ pentagonal bipyramids share opposite equatorial edges to form mono-dimensional $^1_\infty[U(2)O_5]$ zig-zag chains. $V(1)O_4$ tetrahedral are attached on both sides of the chains forming $^1_\infty[U(2)V(1)O_7]$ ribbons with *mm* symmetry running down the *a*- or *b*-axis of the tetragonal unit cell.

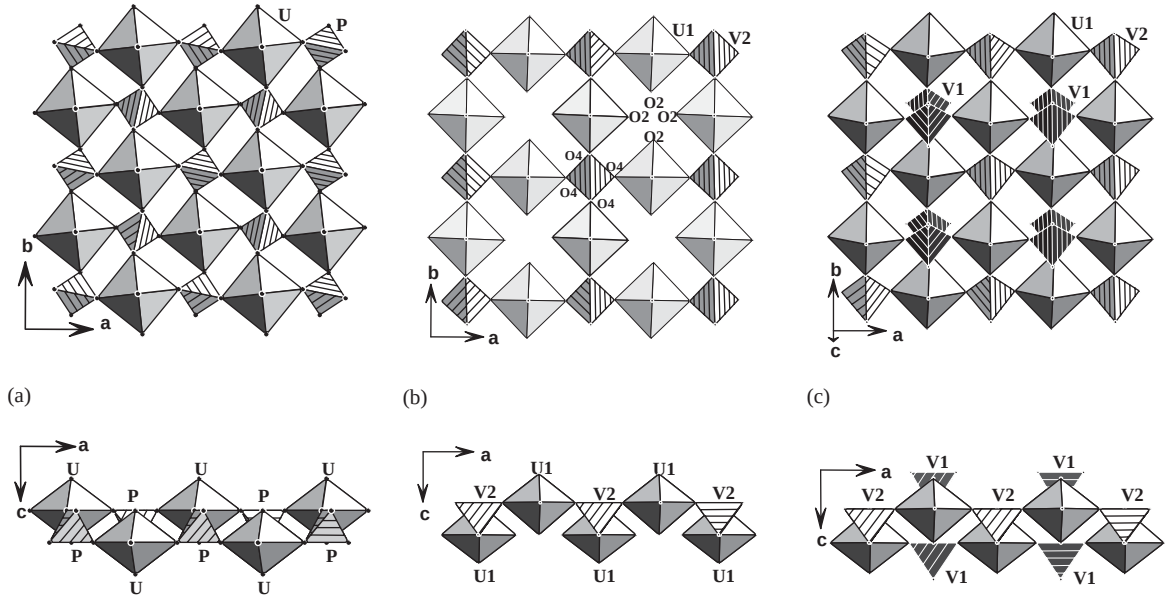

Fig. 3. In HUP and $Na(UO_2)_4(VO_4)_3$, one quarter of the squares of the anion-topology that contains only squares is occupied by UO_6 octahedra. In HUP one other quarter is populated by PO_4 tetrahedra (a), in $Na(UO_2)_4(VO_4)_3$ one eighth is occupied by $V(2)O(4)_4$ tetrahedra (b), when $V(1)O_4$ tetrahedra are attached above and below the empty sites (c).

that localize the heavy atoms, U and V. The positions of sodium and oxygen atoms were deduced from subsequent refinements and difference Fourier syntheses. The atomic scattering factors for neutral atoms were taken from the "International Tables for X-ray Crystallography" [25]. Refinement results of the atomic coordinates and anisotropic displacement parameters are listed in Tables 4 and 5, respectively. The most significant inter-atomic distances with metal to oxygen, bond valences and uranyl angles are reported in Table 6. Bond valences were calculated using Brese and O'Keeffe data [26] with $b = 0.37$ Å except for U–O bonds where the coordination independent parameters ($R_{ij} = 2.051$ Å, $b = 0.519$ Å) were taken from Burns et al. [27].

2.3. Electrical conductivity measurements and thermal analyses

Electrical conductivity measurements were carried out on cylindrical pellets (diameter, 5 mm; thickness, ca. 3.5 mm) obtained using a conventional cold press and sintered at 700°C for 2 days, followed by very slow cooling, 5°C/h, until room temperature. Gold electrodes were vacuum-deposited on both flat surfaces of the pellets. Conductivity measurements were performed by ac impedance spectroscopy over the range 1–10^6 Hz with a Solartron 1170 frequency-response analyzer. Measurements were made at 20°C intervals over the range 30–700°C on both heating and cooling. Each set of values was recorded at a given temperature after a 1 h

stabilization time. Differential thermal analyses (DTA) were performed in air with a SETARAM 92-1600 thermal analyzer in the temperature range 20–1000°C with heating and cooling rate 1.5°C/min using platinum crucibles. DTA measurements showed that both compounds incongruently melt at 870°C and 850°C for $Na(UO_2)_4(VO_4)_3$ and $Li(UO_2)_4(VO_4)_3$, respectively.

3. Crystal structure description and discussion

There are two symmetrically independent uranium atoms in 8*e* special sites, U(1) with an octahedral coordination of oxygen atoms and U(2) surrounded by seven oxygen atoms in a pentagonal bipyramidal environment. In both cases two oxygen atoms at short distances create an uranyl ion UO_2^{2+}. In the $U(1)O_6$ octahedron, the uranyl ion is perfectly linear but with two different U–O bond lengths, U(1)–O(1) = 1.877(10) Å and U(1)–O(3) = 1.790(14) Å. In the equatorial plane, the oxygen atoms O(2) and $O(2)^i$, as O(4) and $O(4)^i$ are symmetrically related, at 2.230(9) and 2.196(10) Å, respectively. In the $U(2)O_7$ pentagonal bipyramids, the O(6)–U(2)–$O(6)^{ii}$ uranyl ion is also nearly linear (179.4(4)°) and admits the equatorial pentagon plane as a mirror, the distances being equal to 1.745(9) Å and shorter than those of $U(1)O_2^{2+}$ ion. In the equatorial plane, two pairs of oxygen atoms [$O(5)^{iii}$, $O(5)^{iv}$) and ($O(5)^{vi}$, $O(5)^{vii}$] are situated at 2.347(9) and 2.461(10) Å, respectively, the fifth oxygen atom $O(1)^v$ being at an intermediate distance 2.397(10) Å.

The two independent vanadium atoms V(1) and V(2) are situated in 8*e* and 4*b* special sites, respectively, with a tetrahedral environment of oxygen atoms. The $V(2)O_4$ is nearly perfect with four V(2)–O(4) distances equal to 1.721(11) Å in agreement with the sum of ionic radii [28] and four bonds angles of 108.7(1)° and the two others of 111.0(5)°. The $V(1)O_4$ tetrahedron is more distorted, the V(1) atom is displaced towards the O(2)–O(2) edge leading to two short V(1)–O(2) bonds of 1.666(10) Å and two quite usual V(1)–O(5) bond lengths of 1.719(10) Å, and accordingly to high O(2)–V(1)–O(2) angle of 112.5(5)° and a low O(5)–V(1)–O(5) angle of 96.9(5)°.

The $U(2)O_7$ pentagonal bipyramids shared opposite edges O(5)–O(5) to form infinite zig-zag chains $^1_\infty[U(2)O_5]$, Fig. 2, running down the *b*-axis at $z\sim0$ and $z\sim\frac{1}{2}$ and down the *a*-axis at $z\sim\frac{1}{4}$ and $z\sim\frac{3}{4}$, Fig. 4. These chains are similar to those found in numerous uranyl-containing compounds but it is the first example of $^1_\infty[U(2)O_5]$ chains running down two perpendicular directions. In all the other compounds the chains are parallel to each other and connected by non-shared oxygen atoms or through various polyhedra to form bi-dimensional planar or corrugated layers (see, for example, Ref. [18]). In $Na(UO_2)_4(VO_4)_3$, $V(1)O_4$ tetrahedra are linked to either side of the $^1_\infty[U(2)O_5]$ chains

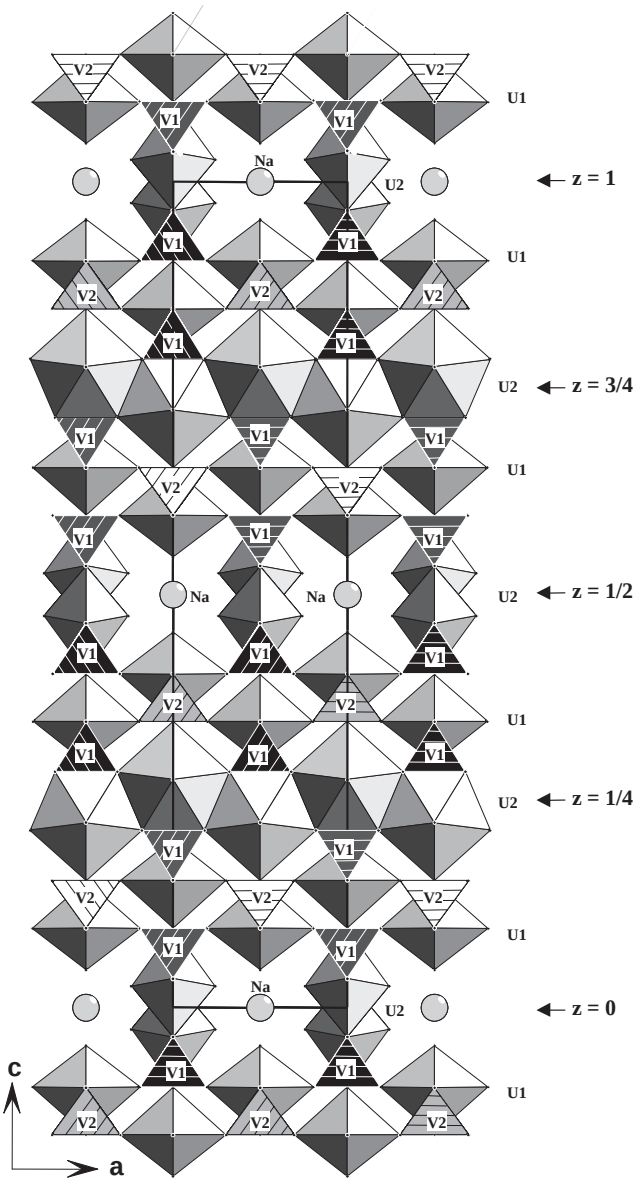

Fig. 4. In $Na(UO_2)_4(VO_4)_3$ the three-dimensional arrangement of UO_7 pentagonal bipyramids, UO_6 octahedra an VO_4 tetrahedra creates non-crossing one-dimensional tunnels running both down *a*- and *b*-axis of the tetragonal unit cell and populated by Na^+ ions.

by sharing the O(5)–O(5) edges with the $U(2)O_7$ polyhedra to form $^1_\infty[U(2)V(1)O_7]$ ribbons that possess two mirror symmetry planes parallel to (100) and (010), Fig. 2. According to the theory of Pauling [29] and Bauer [30], the O(5)–O(5) edge shared between VO_4 and UO_7 polyhedra is shorter [2.573(13) Å] than the other O–O edges which are not shared and participates to the lowering of the O(5)–V(1)–O(5) angle.

The $U(1)O_6$ and $V(2)O_4$ polyhedra are corner shared to form sheets parallel to (001), Fig. 3b. A $V(2)O_4$ tetrahedron shares its four O(4) corners with four different $U(1)O_6$ distorted octahedra, the uranyl bonds being perpendicular to the sheet. The sheets are based

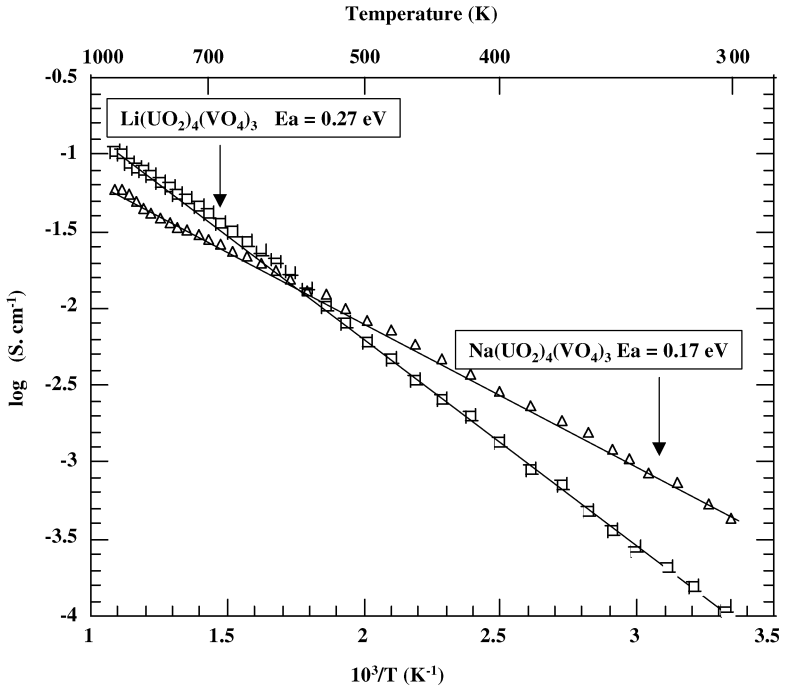

Fig. 5. Conductivity Arrhenius plots for $Na(UO_2)_4(VO_4)_3$ and $Li(UO_2)_4(VO_4)_3$.

upon the anion-topology that contains only squares described by Burns et al. [1] in which one quarter of the squares are populated by UO_6 octahedra and one eighth are populated by VO_4 tetrahedra, giving a sheet with the composition ${}^2_\infty[(UO_2)_2(VO_4)]^+$. The same anion-topology exists in $H(UO_2)(PO_4)\cdot 4H_2O$, named HUP [31], which is among the best electrical proton conductors known currently, and in the $M(UO_2)(PO_4)\cdot nH_2O$ ($M=$ Li, Na, K, NH_4, $\frac{1}{2}$Ca) [32] analogs, in which one half of the squares are populated, one quarter with UO_6 octahedra and one quarter with PO_4 tetrahedra, giving sheets with the composition ${}^2_\infty[(UO_2)(PO_4)]^-$ (Fig. 3a), the water molecules and the cations being in the space between the sheets. In fact the bi-dimensional arrangement of UO_6 octahedra creates tetrahedral sites formed by the equatorial oxygen atoms. In HUP all the sites are occupied by P atoms, on the contrary in $Na(UO_2)_4(VO_4)_3$ half tetrahedral sites, formed by O(4) atoms, are occupied by V(2) while the other half, formed by O(2) atoms, are empties (Fig. 3b). The $V(1)O_4$ tetrahedra are attached above and below these empty sites to form ${}^2_\infty[(UO_2)_2(VO_4)_3]^{5-}$ sheets, thus, above the sheet, all the non-shared O(2)–O(2) edges are parallel to the [010] direction when, below the sheet, they are parallel to the [100] direction, Fig. 3c. The $V(1)O_4$ tetrahedra and the O(1) atoms are shared between the ${}^2_\infty[(UO_2)_2(VO_4)_3]^{5-}$ sheets parallel to (001) and the ${}^1_\infty[U(2)V(1)O_7]$ ribbons to form a tri-dimensional framework creating nearly circular channels running alternately down [010] and [100] directions and limited only by uranyl oxygen ions, Fig. 4. The tunnels result from face-shared $O(6)_4O(3)_2$ distorted octahedra, the Na^+ ion half occupy the octahedral sites. Thus, the Na^+ ions are surrounded by six uranyl-oxygen atoms, two O(3) atoms at 2.388(9) and four O(6) at 2.746(7). The role of O(1) is particular, it acts as an uranyl oxygen for U(1) and as an equatorial oxygen for U(2). Such oxygens exist, for example, in anhydrous uranyl compounds of the family UO_2XO_4 with $X=$ S, Cr, Se, Mo and W [33–36] which adopt the same crystal structure which results from the association of $(UO_2)O_5$ pentagonal bipyramids sharing four equatorial oxygen atoms with four different XO_4 tetrahedra, the last equatorial oxygen atom being shared with an apical oxygen atom of a neighboring $(UO_2)O_5$ bipyramid.

Bond valence sums calculation provides values of 5.985, 6.159 and 5.004 v.u. for U(1), U(2) and V(2), respectively, which are consistent with formal valences U^{6+} and V^{5+}. On the contrary, due to the strong V(1)–O(2) bonds, the V(1) atom appears over-bonded. The Na^+ ion disordered on the distorted octahedral sites forming the channels are under-bonded. For oxygen atoms the calculated valence bond sums ranged from 1.915 to 2.276 with an average value of 2.063, showing that the oxygen atoms are only in the ion oxide form.

The partial occupation of the Na^+ sites should be favorable for a good cationic electrical conductivity, thus, ionic conductivity measurements for both isotypic compounds $M(UO_2)_4(VO_4)_3$ ($M=$ Li, Na) were made and reported in Fig. 5. For both compounds an Arrhenius law applies for the whole temperature range

explored with activation energy of 0.17 and 0.27 eV for Na and Li compounds, respectively. For the Na compound the activation energy is comparable to the reported value for sodium β-alumina (0.15 eV) [37] and lower than the value for the sodium ion conductor Nasicon, $Na_3Zr_2PSi_2O_{12}$ (0.33 eV) [38]. The activation energy for the Li compound is significantly higher, in fact the octahedral sites are too large for Li^+ and we can suppose that the Li^+ ion tends to stick at sites in the channel walls, as already mentioned for Li^+ β-alumina [37]. However, the activation energy for electrical conductivity is comparable to the value reported for the best lithium ion conductor Li_3N (0.25 eV) [39] and lower than the values for Lisicon, $Li_{14}ZnGe_4O_{16}$, below 250°C (0.56 eV) [40] and for $Li_{3.5}Si_{0.5}P_{0.5}O_4$ (0.52 eV) [41]. At low temperature, the conductivity of $Na(UO_2)_4(VO_4)_3$ is comparable to that of Nasicon and lower than that of Na^+ β-alumina, Fig. 6. The conductivity of $Li(UO_2)_4(VO_4)_3$ is much higher than that of Li^+ β-alumina [37] and lower than that of Lisicon, except at low temperature where the conductivities are comparable. The high ionic conductivity in $M(UO_2)_4(VO_4)_3 (M = Li, Na)$ compounds may be due to the migration of the M^+ ions in the mono-dimensional channels that run down to two perpendicular directions. This is different from the other sodium or lithium ion conductors based on layers (β-alumina) or intersecting open channels (Nasicon and Lisicon). However, in the present class of materials the exact mechanism for conduction is presently not known and further experiments are needed.

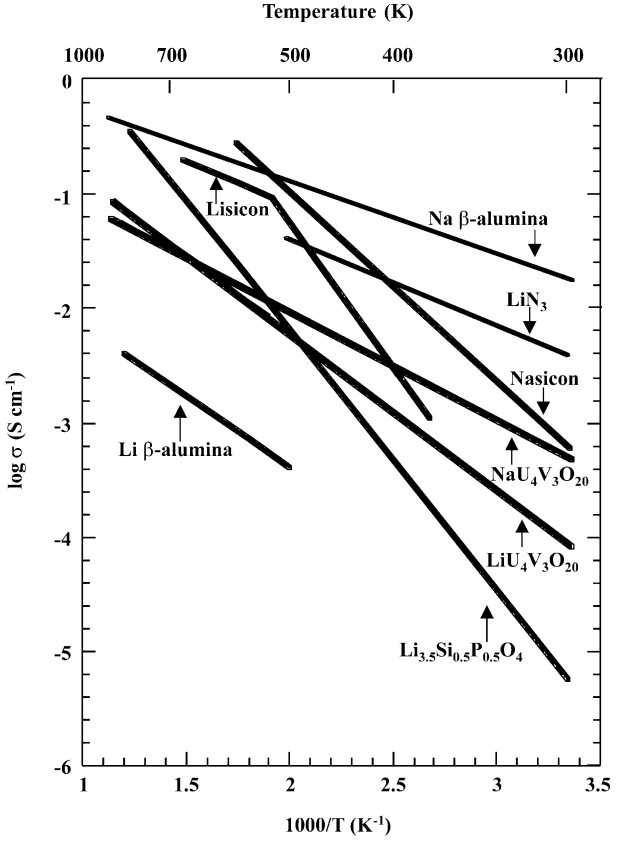

Fig. 6. Comparison of Conductivity of $M(UO_2)_4(VO_4)_3$ compounds with other well-known fast sodium or lithium ions conductors.

References

[1] P.C. Burns, M.L. Miller, R.C. Ewing, Can. Mineral. 34 (1996) 845.
[2] F. Abraham, C. Dion, M. Saadi, J. Mater. Chem. 3 (5) (1993) 459.
[3] M. Saadi, Thesis, Lille, 2001.
[4] F. Abraham, C. Dion, N. Tancret, M. Saadi, Adv. Mater. Res. 1–2 (1994) 511.
[5] P.B. Barton, J. Am. Miner. 43 (1958) 799.
[6] D.E. Appleman, H.T. Evans, J. Am. Miner. 50 (1965) 825.
[7] P.G. Dickens, G.P. Stuttard, R.G.J. Ball, A.V. Powell, S. Hull, S. Patat, J. Mater. Chem. 2 (2) (1992) 161.
[8] J. Borène, F. Cesbron, Bull. Soc. Fr. Miner. Crystallogr. 93 (1970) 426.
[9] J. Borène, F. Cesbron, Bull. Soc. Fr. Miner. Crystallogr. 99 (1971) 8.
[10] D.P. Shashkin, Dokl. Akad. Nauk SSSR 220 (1974) 1410.
[11] P. Piret, P. Declercq, D. Wauters-Stoop, Bull. Miner. 103 (1980) 176.
[12] I. Duribreux, C. Dion, M. Saadi, F. Abraham, J. Solid State Chem. 146 (1999) 258.
[13] A.M. Chippinade, S.N. Crennell, P.G. Dickens, J. Mater. Chem. 3 (1993) 33.
[14] C. Dion, S. Obbade, E. Raekelboom, M. Saadi, F. Abraham, J. Solid State Chem. 155 (2000) 342.
[15] S. Obbade, C. Dion, L. Duvieubourg, M. Saadi, F. Abraham, J. Solid State Chem. 173 (2003) 1.
[16] A.M. Chippinade, P.G. Dickens, G.J. Flynn, G.P. Stuttard, J. Mater. Chem. 5 (1) (1995) 141.
[17] N. Tancret, S. Obbade, F. Abraham, Eur. J. Solid State Inorg. Chem. 32 (1995) 195.
[18] M. Saadi, C. Dion, F. Abraham, J. Solid State Chem. 150 (2000) 72.
[19] S. Obbade C. Dion, M. Saadi, F. Abraham, J. Solid State Chem., (2004) in press.
[20] G. Smith, R.J. Snyder, J. Appl. Crystallogr. 12 (1979) 60.
[21] SAINT Plus Version 5.00, Bruker Analytical X-ray Systems, Madison, WI, 1998.
[22] G.M. Sheldrick, SHELXTL NT, Program Suite for Solution and Refinement of Crystal Structure Version 5.1, Bruker Analytical X-ray Systems, Madison, WI, 1998.
[23] R.H. Blessing, Acta Crystallogr. A 51 (1995) 33.
[24] G.M. Sheldrick, SHELXS-86, Program for Crystal Structure Determination, University of Göttingen, Germany, 1986.
[25] J.A. Ibers, W.C. Hamilton (Eds.), International Tables for X-ray Crystallography, Vol. IV, Kynoch Press, Birmingham, UK, 1974.
[26] N.E. Brese, M. O'Keeffe, Acta Crystallogr. B 47 (1991) 192.
[27] P.C. Burns, R.C. Ewing, F.C. Hawthorne, Can. Mineral. 35 (1997) 1551.
[28] R.D. Shannon, Acta Crystallogr. A 32 (1976) 751.
[29] L. Pauling, The Nature of the Chemical Bond, Vol. 5, 3rd Edition, Cornell University Press, Ithaca, 1960, p. 547.
[30] W.H. Bauer, Am. Mineral. 57 (1972) 709.
[31] B. Morosin, Acta Crystallogr. B 34 (1978) 3732.

[32] C.M. Johnson, M.G. Shilton, A.T. Howe, J. Solid State Chem. 37 (1981) 37.
[33] L.M. Kovba, V.K. Trunov, A.J. Grigorev, Zh. Strukt. Khim. 6 (1965) 919.
[34] V.N. Serezhkin, V.V. Tabachenko, L.B. Serezhkina, Radiokhimiya 20 (1978) 214.
[35] V.N. Serezkhin, L.M. Kovba, V.K.T runov, Kristallografiya 6 (1972) 1127.
[36] V.N. Serezkhin, L.M. Kovba, L.G. Mokarevitch, Kristallografiya 25 (1980) 858.
[37] M.S. Whittingham, R.A. Huggins, Solid State Chem., in: R.S. Roth, S.J. Scheneider (Eds.), Nat. Bur. Standards Spec. Pub., Vol. 364, 1972, p. 139.
[38] K.D. Kreuer, H. Kholer, J. Maier, High Conductivity Solid Ionic Conductors, World Scientific Publishing, Singapore, 1989, p. 242.
[39] U.V. Alpen, A. Rabenau, G.H. Talat, App. Phys. Lett. 30 (12) (1977) 621.
[40] H.Y.-P. Hong, Mater. Res. Bull. 13 (1978) 117.
[41] Y.W. Hu, I.D. Raistrick, R.A. Huggins, J. Electrochem. Soc. 124 (1977) 1240.